Artificial Intelligence In Medicine 136 (2023) 102477

Contents lists available at ScienceDirect

Artificial Intelligence In Medicine

journal homepage: www.elsevier.com/locate/artmed

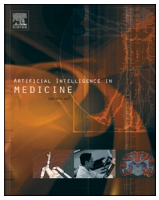

An intelligent non-invasive system for automated diagnosis of anemia exploiting a novel dataset

Giovanni Dimauro [a,*], Maria Elena Griseta [b], Mauro Giuseppe Camporeale [a], Felice Clemente [c], Attilio Guarini [c], Rosalia Maglietta [b]

[a] Department of Computer Science, University of Bari 'Aldo Moro', Bari, Italy
[b] Institute of Intelligent Industrial Technologies and Systems for Advanced Manufacturing, National Research Council of Italy, Bari, Italy
[c] Haematology Dept. of National Cancer Institute 'Giovanni Paolo II', Bari, Italy

ARTICLE INFO

Keywords:
Machine learning
Anemia
RUSBoost
Unbalanced dataset
Non-invasive techniques

ABSTRACT

Anemia is a condition in which the oxygen-carrying capacity of red blood cells is insufficient to meet the body's physiological needs. It affects billions of people worldwide. An early diagnosis of this disease could prevent the advancement of other disorders. Traditional methods used to detect anemia consist of venipuncture, which requires a patient to frequently undergo laboratory tests. Therefore, anemia diagnosis using noninvasive and cost-effective methods is an open challenge. The pallor of the fingertips, palms, nail beds, and eye conjunctiva can be observed to establish whether a patient suffers from anemia.

This article addresses the above challenges by presenting a novel intelligent system, based on machine learning, that supports the automated diagnosis of anemia. This system is innovative from different points of view. Specifically, it has been trained on a dataset that contains eye conjunctiva photos of Indian and Italian patients. This dataset, which was created using a very strict experimental set, is now made available to the Scientific Community.

Moreover, compared to previous systems in the literature, the proposed system uses a low-cost device, which makes it suitable for widespread use.

The performance of the learning algorithms utilizing two different areas of the mucous membrane of the eye is discussed. In particular, the RUSBoost algorithm, when appropriately trained on palpebral conjunctiva images, shows good performance in classifying anemic and nonanemic patients. The results are very robust, even when considering different ethnicities.

1. Introduction

ANEMIA is a global public health problem that affects people in both developing and developed countries and has significant consequences for human health, such as a reduction in the concentration of blood hemoglobin (Hb). The World Health Organization (WHO) reports that more than one billion people worldwide are affected by anemia of varying degrees of severity [1–6]. From a clinical perspective, anemia is a condition in which the number of red blood cells or the Hb concentration within them is lower than normal. Hb is needed to carry oxygen, and if a patient lacks red blood cells or Hb or has abnormal red blood cells, there is a decrease in the capacity of the blood to carry oxygen to the body's tissues. This results in symptoms such as tiredness, weakness, dizziness, and shortness of breath. Anemia caused by iron, vitamin B12, folate, or Hb deficiencies results in abnormal or otherwise different erythrocyte production patterns [7]. Normally, no clear symptoms appear when Hb is >9–10 g/dL because the body attempts to compensate for this loss. For example, an increase in heart rate occurs in response to hypoxia. When this compensation can no longer provide an adequate level of oxygen, the aforementioned symptoms appear.

As described by the WHO [1], complete and reliable detection of anemia worldwide along with determination of its overall consequences is extremely difficult, even in more economically advanced areas. What is certain is that anemia is a disease that greatly impacts the world population, with major consequences for social and economic development. All countries must bear the costs of coping with this disease:

* Corresponding author.
E-mail addresses: giovanni.dimauro@uniba.it (G. Dimauro), mariaelena.griseta@stiima.cnr.it (M.E. Griseta), mauro.camporeale@uniba.it (M.G. Camporeale), felice.clemente.irccsbari@gmail.com (F. Clemente), attilioguarini@oncologico.bari.it (A. Guarini), rosalia.maglietta@cnr.it (R. Maglietta).

https://doi.org/10.1016/j.artmed.2022.102477
Received 25 August 2022; Received in revised form 19 December 2022; Accepted 19 December 2022
Available online 26 December 2022

prevention (or failure to prevent), instrumentation for traditional analysis, administration, and accommodation. Furthermore, it is impossible to estimate the financial and social costs for patients with anemia. In fact, some patients must frequently undergo laboratory testing, which can be uncomfortable due to frequent blood draws and incur additional costs for transportation and/or assistance. Additionally, mass screening is impossible in developing countries, especially in geographic areas with limited economic resources, owing to the lack of noninvasive and cost-effective diagnostic techniques.

To obtain a definitive diagnosis, a careful study of the patient's medical history as well as physical and instrumental examinations are needed. During the physical examination, the heart and respiratory rates are collected, and the pallor of exposed tissues is evaluated [8–14]. Blood sample analysis is then used to provide a definitive diagnosis of anemia. A number of studies have been conducted to establish whether the direct examination of the exposed tissue by the physician is sufficiently reliable to determine anemia. The results are rather controversial, but many authors agree that the estimate is reliable only for cases of severe anemia and that the result depends on doctor's experience and the use or non-use of aids as color-tint selectors [14,15].

In the last decade, many researchers have expressed growing interest in the methods and tools used to monitor the concentration of Hb in noninvasive and cost-effective ways for both laboratory and at-home use [16]. Doctors can suspect anemia by observing the palms of the hands, fingertips, nail beds, and eye conjunctiva [17–49], but the diagnosis cannot be certain. Therefore, it is essential to develop devices and methods that can diagnose anemia by acquiring images of these areas of the body in a noninvasive, cost-effective, and easily accessible manner [39]. Machine learning techniques have been widely and successfully applied in many fields [50–54], particularly medicine [55–66], as well as in anemia assessment [24,25,67–69].

Research on the automatic diagnosis of anemia through non-invasive techniques began a few years ago; therefore, no shared datasets are available on which to compare different approaches. Moreover, some issues are controversial; for example, the threshold values for anemia defined by the WHO are a subject of extensive discussion. In recent years, various studies on the use of exposed tissues to assess the state of anemia have presented various techniques and reported promising results. One crucial point is that each research group worked on their own data, sometimes on very small datasets or without specifying the experimental set, and without paying particular attention to non-trivial problems such as the influence of ambient light during image capture. Furthermore, the equipment utilized in certain research is complex and costly, making it unsuitable for large-scale industrial development.

In [70], the authors summarized several open problems: a) which part of the conjunctiva guarantees better results in estimating anemia; b) how many digital images of one or both eyes are sufficient for a reliable evaluation; c) the lack of a shared dataset; and d) the lack of low-cost devices suitable for widespread use.

This work contributes to some of these open challenges by presenting a novel non-invasive and cost-effective machine learning-based approach to aid in the automated detection of anemia. Moreover, a device and software system designed for widespread use is presented, which has been trained and tested on conjunctiva images from the Eyes-defy-anemia dataset and has shown good performance. This system uses RUSBoost [56,71,72], which is excellent for managing unbalanced class datasets. A valuable contribution of this article is the publication of Eyes-defy-anemia, a novel dataset containing conjunctiva images of Italian and Indian patients. Its descriptions and links are presented in Appendix 1. As a minor contribution, the role of the palpebral and forniceal parts of the conjunctiva has been investigated to establish which part guarantees a higher prognostic or predictive value, with the aim of designing more reliable diagnostic systems.

Interestingly, the availability of several images acquired from patients of two different ethnicities made it possible to evaluate the robustness of the methodology presented here based on the different physical attributes of the patients involved.

The remainder of this paper is organized as follows. The second section describes the existing literature on anemia diagnosis through the analysis of different exposed tissues of the body and cost-effective and noninvasive devices that have already been used by researchers in previous research. In the third section, the two datasets and the proposed statistical methodology for anemia detection are described. Section 4 describes the experiments and discusses the results obtained. The conclusions and bibliographic references are provided in Sections 5 and 6, respectively.

2. State-of-the-art

The first subsection includes a short review of the literature regarding different areas of the body that can be used to diagnose anemia. We then summarize a series of recent studies on noninvasive and cost-effective devices employed to detect anemia in an accessible manner for patients at home or in the laboratory.

2.1. Anemia diagnosis observing different tissues

Many research [8,14,73,74] have demonstrated that the whiteness of exposed regions of the human body may be used to quantify anemia. Pallors are characterized by a lack of color in the skin and mucous membranes due to a low level of circulating Hb. A pallor can affect the entire body, but it is mainly observed in areas where blood vessels are more evident, for example, in mucous membranes such as the tongue or conjunctiva.

The validity of the diagnosis of anemia through the clinical evaluation of the pallor of the exposed areas of the body is evidenced by numerous findings in the literature. As described in [12], the Integrated Management of Childhood Illness suggests observing the color of the palm to diagnose severe anemia. Further tissue evaluation is advised because a greater presence of melanin might impact palm paleness. As a more significant presence of melanin can influence palm paleness, further tissue examination is recommended. The authors showed that it is possible to correctly classify the anemia status of children through examination of conjunctival pallor. Moreover, substantial results were obtained for the observation of fingertips. In addition, many authors have evaluated the correlation between the opinions expressed by different doctors. Various problems have been highlighted, such as differences in ethnic groups, environmental lighting conditions, observer experiences, and the presence of pathologies such as β-thalassemia [13,14,75].

From the results we obtained, we can argue that observing the conjunctiva can ensure greater reliability than observing the palm of the hand or nail beds. The palpebral conjunctiva has a number of benefits over other exposed tissues, including the fact that it is not affected by pathological diseases like fever and is less susceptible to temperature changes(causing vasoconstriction/dilation) than other tissues like the nail bed, the palm, the skin overall, and the fingertips. Paleness estimation in other tissues is influenced by important factors such as melanin, ethnicity, skin folds, discoloration, and nail thickness.

In this article, we consider images of the eye conjunctiva and evaluate the pallor of the mucosa to establish whether a patient is suffering from anemia. We focused our interest on the conjunctiva and compared the results considering only the palpebral or whole conjunctiva, which consists of the forniceal and palpebral. As suggested by the authors in [70], the abundance of microvessels makes the conjunctiva a suitable tissue for anemia detection. The high vascularization of the palpebral conjunctiva in comparison to that of the forniceal conjunctiva most likely emphasizes minimal variations in blood color.

2.2. Cost effective and noninvasive devices employed to diagnose anemia

Researchers have considered whether cost-effective and noninvasive

personal medical systems based on artificial intelligence can be employed in healthcare and medical services. A significant number of noninvasive anemia assessment studies have been published since 2014, with India, the USA, and China contributing the most research. According to two of these studies, anemia is most common in pregnant women and preschool children [1]. Another study revealed that reducing healthcare costs could be of particular relevance in the USA [16].

The majority of anemia detection device research has focused on the indirect assessment of Hb levels in the blood and the level of oxygen in human tissues [16,76,77]. Pulse co-oximeters employ light reflection qualities to discriminate between oxyhemoglobin and deoxyhemoglobin, and digital cameras are used to capture images or movies. In addition, devices that require a small drop of blood can evaluate Hb, and smartphones are used as a measurement tool and user-friendly service to monitor patients' conditions.

Some commercially available techniques include photoplethysmography, reflectance spectroscopy, and fluorescence spectroscopy of oral tissue; however, many of these techniques are not affordable, portable, or wearable [32,78].

The finger is the most-analyzed body part. Devices and technologies can extract data from fingertip capillaries owing to the considerable use of co-oximeters, which in most cases use a finger clamp to extract data [16,79,80]. Certain cameras and smartphone devices are also used to capture pictures or small videos of the fingertip. The conjunctiva has also been studied extensively. Other parts of the body, such as the fingernails, eye sclerae, retinas, palms of the hands, tongue, and lips, were sampled to a lesser extent.

In [81], the conjunctiva image was taken with a personal digital assistant, which corrected the variation in ambient light through a standard gray card acquired with the eye image. The images were then processed on a computer. Additionally, [40] considered ambient light, and a comparison between digital camera and smartphone camera images was carried out. The image colors were standardized using a color calibration card; however, the effect of ambient lighting was not completely eliminated. The acquisition of raw images is also suggested to avoid the impact of filters automatically applied by the acquisition device software.

In [41], the calibration of digital images was performed to reduce the impact of ambient light on the area of the eyelid conjunctiva. This was accomplished using the Mahalanobis distance, a texture-based feature, and two color-based features. Classification was performed using a support vector machine and an artificial neural network. The authors described a sensible reduction in the residual indecision of previous studies using the Kalman filter, as explained in [42]. In [43], a device was presented to eclipse external light sources. A standard viewer with internal lighting and an internal smartphone were used to acquire images of the conjunctiva. The device was improved in [36,39]. The new device uses a special spacer and macro lens to obtain close-up images with a high-resolution smartphone. Internal LED lighting ensures image color standardization. The eye area could be freely photographed at a close range with the certainty of causing no harm to the patient. There are demonstrations in the literature that indicate that the LED lights used by smartphones cannot damage the delicate human visual system in any way [82]. The authors in [39] also presented software that allows the acquisition of eye images, assisted selection of the conjunctiva region, and estimation of the condition of anemia. It is designed to store patient data that can then be assessed or sent to a doctor.

In [38,83], two studies were presented with the goal of providing health resources to developing countries, where it is difficult to diagnose anemia using traditional methods. In the latter study, the problem of postpartum hemorrhage caused by anemia, which occurs mainly in Africa and Asia, was discussed. Both studies were based on the analysis of the color of the conjunctiva; in particular, in the latter study, photos were taken in ambient lighting by utilizing the camera of the Asus ZenFone 2 Laser smartphone without flash and using white paper positioned next to the eye to standardize white.

More recently, researchers have applied sophisticated techniques to correlate conjunctival color with Hb levels. In [37], the k-means algorithm was used to group the homogeneous color pixels extracted from the conjunctival images, thereby increasing the accuracy of anemia estimation. In [84], the authors concluded that using a previously trained Elman neural network allows the effective classification of anemic and non-anemic patients.

Another interesting study was published in [82]. The authors introduced virtual hyperspectral imaging (VHI), which virtually transforms a built-in camera (i.e., RGB sensor) in a smartphone into a hyperspectral imager and combines the imaging of peripheral tissue with spectroscopic quantification of Hb to obtain good performance.

Finally, considerable interest has been devoted to segmentation. Some experiments were performed by manually segmenting the region of interest (ROI), which is the portion of the conjunctiva considered for pallor evaluation. In [85], the eye region was automatically segmented through iterative use of the Viola-Jones algorithm. This approach involves improving the image quality and applying algorithms that extract the area of interest. In [86–88], new approaches were presented to segment the conjunctiva, with fascinating results. In this study, all conjunctiva images, whole and palpebral, were segmented manually. Table 1 shows a comparison between some of the above-presented studies in terms of the used classifier and achieved metrics, showing at a glance what has been achieved by the scientific community in this field, but has little significance in terms of comparing results because each experiment was performed on different datasets, collecting different images (e.g., in terms of environmental conditions and ROIs), with different numbers of classes and different inter-class balance.

3. Materials and methods

3.1. Description of the datasets

The dataset Eyes-defy-anemia contains 218 photos of eyes, of which

- A total of 123 eye images from Italian patients were acquired along with a blood sample. In the following experiments, among the Italian patients, Patient 93 was discarded because his/her Hb concentration was missing; Patients 1, 35, 54, 58, and 109 were not included because their forniceal conjunctivas were not exposed in the images. Therefore, 116 patient eye images were considered and labeled as the Italian dataset.
- Ninety-five eye images belonging to Indian patients were acquired in Karapakkam, Chennai (India), together with blood samples, and labeled as the Indian dataset.

Patients in both groups had a routine blood draw, and on that

Table 1
Comparison between other methods to detect anemia. Keys: SVM (support vector machine), ANN (artificial neural network), LR (linear regression), DT (decision tree), k-NN (k nearest neighbors), LS-SVM (least squares support vector machine), LR (linear regression), R (regression), MLR (multivariate linear regression), kM (k-means).

Paper	Classifier	Accuracy	Specificity	Sensibility
Sevani [36]	kM	0.9	–	–
Tamir [37]	–	0.79	–	–
Chen [40]	SVM	0.32	0.9	0.62
Chen [40]	ANN	0.81	0.83	0.78
Chen [41]	R	–	–	–
Bevilacqua [42]	SVM	0.84	0.82	1
Suner [74]	–	0.71	0.72	0.69
Anggraeni [76]	LR	–	–	–
Muthalagu [77]	ANN	–	0.96	0.94
Irum [78]	LS-SVM	0.85	0.7	0.92

occasion, we asked for their consent to take a picture of the conjunctiva and to record the Hb value determined in the laboratory. All patients agreed to the informed consent form; no patients disclosed any underlying diseases; and no personal information was collected. The study was conducted according to the principles of the Declaration of Helsinki.

The device (Fig. 1), described later, was used to acquire eye images of Indian and Italian patients. All photographs were acquired at the same distance and with the same white LED light. From these images, both the palpebral conjunctiva and the whole (forniceal and palpebral) conjunctiva were considered and either automatically segmented or manually segmented by experts (Fig. 2). All images obtained after segmentation were RGB images of equal size (1067 × 800 pixels).

Each dataset was accompanied by an Excel file that reported patient data, which included demographic information, such as sex and age, and medical information, such as the Hb concentration level obtained by the blood count, expressed in g/dL. Approximately 48 % and 33 % of the Indian and Italian patients, respectively, were female. The average age of the patients was 34 years (respectively 49), with a range of 19–75 (respectively 20–88) in Indian (respectively Italian) patients. In addition, the Excel file of the Italian patients notes the six patients for whom the forniceal conjunctiva is not visible and the patient whose Hb concentration is missing. All the images were captured by a Samsung S6 smartphone, which is a cost-effective device equipped with a device that enlarges images, standardizes lighting, and removes the influence of ambient light.

In addition, we consider the common dataset, composed of both Indian and Italian patient eye image datasets and thus composed of 211 images (see Fig. 3 for details), using both palpebral conjunctivas and the whole (forniceal and palpebral) conjunctivas.

To determine whether a patient was anemic, we used an Hb concentration threshold value of 10.5 g/dL, as described in [39,43]. More precisely, we considered patients with Hb concentrations less than or equal to 10.5 g/dL to belong to the anemic class, and patients with Hb values >10.5 g/dL to belong to the nonanemic class. Therefore, the Indian and Italian patient eye image datasets included 31 (approximately 33 %) and 11 (approximately 9 %) patients with anemia and 64 (approximately 67 %) and 105 non-anemic patients (approximately 91 %), respectively (see Fig. 3). In contrast, the combined dataset included 42 (approximately 20 %) patients with anemia.

3.2. Features extraction

Eleven features are extracted: $mean_r$, $mean_g$, $mean_b$, *HHR*, *Ent*, *B*, g_1, g_2, g_3, g_4, and g_5. The definitions of these terms are as follows.

The color of the conjunctiva is an indicator of the presence of anemia; the higher the pallor of the conjunctiva, the greater the probability that the patient is anemic. Therefore, some features are extracted from the RGB color space, that is, the mean intensity values of the red ($mean_r$), green ($mean_g$), and blue ($mean_b$) components of the ROI [26]. For each pixel of the ROI, we considered the average of the difference between the red and green components, denoted by $mean_{r-g}$ and described by the following formula:

$$mean_{r-g} = mean(r_i - g_i), \tag{1}$$

where r_i and g_i represent the red and green components of the ith pixel of the segmented conjunctival image [89], respectively.

Following [41], three features were extracted from the dataset that considers the HSI color model, where H, S, and I represent the hue, saturation, and intensity, respectively. Then, a feature called the high hue ratio (*HHR*) is extracted, which represents the proportion of pixels with high values in the hue component of the image and can be expressed as follows:

$$HHR = \frac{n_H}{N}, \tag{2}$$

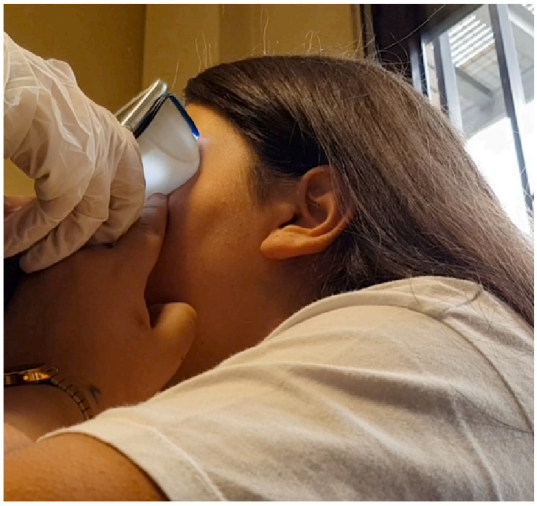

Fig. 1. Conjunctiva acquisition.

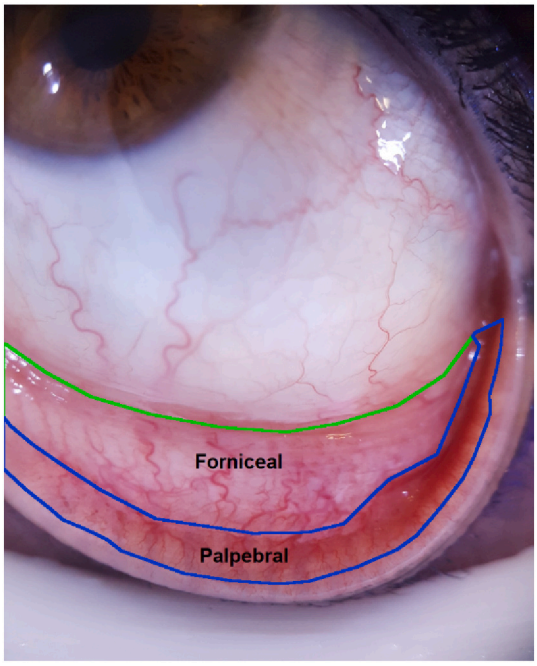

Fig. 2. Forniceal and palpebral conjunctiva.

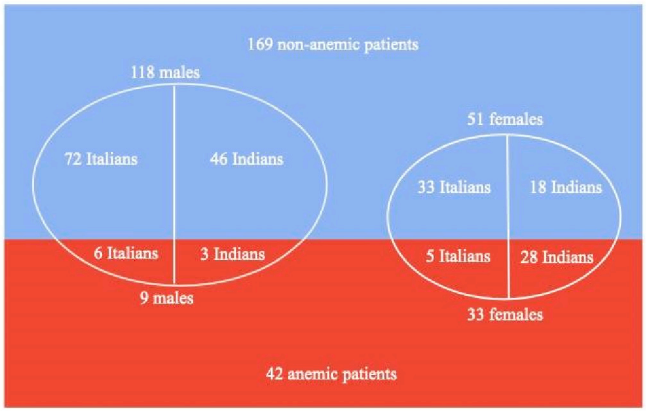

Fig. 3. Description of the Italian and Indian patient eye image datasets based on the patient's sex and ethnicity.

where n_H represents the number of high-hue pixels in an ROI, with a total of N pixels. A high HHR value denotes a large red area in an image. The conjunctiva image of a non-anemic patient tended to have a larger HHR value. We choose, based on empirical evidence, 0.95 as the threshold for high-hue pixels, and in Eq. (2), n_H denotes the number of pixels for which the H component is >0.95.

The conjunctival image of a patient with anemia appears pale white, making the capillaries easier to observe. Therefore, different entropy values can indicate different textures and blood-vessel distributions. Entropy (Ent) is defined as follows:

$$Ent = -\sum_i P(X_i)\, log_2 P(X_i), \tag{3}$$

where $P(X_i)$ represents the estimated occurrence probability of the i-th gray level X_i from the histogram of the image after histogram equalization and $P(X_i) \neq 0$ [41].

Feature B denotes the brightness given by the average grayscale of the image. More precisely

$$B = \frac{\sum_{i=1}^{N} grey_i}{N}. \tag{4}$$

Here, $grey_i$ represents the gray level for the i-th pixel of the ROI image, and N is the total number of pixels.

Finally, an alternative method for diagnosing anemia is to observe the blood vessels of the conjunctiva. In the conjunctival image of anemic patients, blood vessels should be less accentuated than in the image of healthy patients because the blood is lighter in color. In [90,91], the authors proposed a method for blood vessel segmentation to implement pixel-wise classification by computing a feature vector comprising statistical (gray-level) features. Based on the existing literature, we suppose that these gray-level features could help classify images of the conjunctiva of anemic patients based on the increased evidence of blood vessels. Therefore, after computing the gray-level features g_1, g_2, g_3, g_4, and g_5 for each pixel of the ROI as described below, we compute their average on all the pixels of the ROI to acquire five features for each image of the dataset. Gray-level features are based on the differences between the gray level in the candidate pixel of the blood vessel and a statistical value representative of its surroundings. We consider the grayscale image of the segmented conjunctiva and observe that blood vessels appear darker (have lower gray levels) than their surroundings. Hence, we applied a sliding window of size 3 × 3 pixels with a stride of 1 over the grayscale ROI to calculate the following features for each pixel of the conjunctiva image:

$$g_1(x,y) = I(x,y) - \min_{(s,t)\in S^3_{x,y}} \{I(s,t)\}. \tag{5}$$

Eq. (5) represents the difference between the gray intensity level $I(x, y)$ at pixel coordinates (x,y) and the minimum intensity within the 3 × 3 window $S^3_{x,\,y}$ centered in pixel (x,y) to enhance the blood vessel with respect to the background.

$$g_2(x,y) = \max_{(s,t)\in S^3_{x,y}} \{I(s,t)\} - I(x,y). \tag{6}$$

Eq. (6) represents the difference between the maximum gray intensity within the window and the pixel intensity at coordinates (x,y) to enhance the background with respect to the blood vessel.

$$g_3(x,y) = I(x,y) - \operatorname*{mean}_{(s,t)\in S^3_{x,y}} \{I(s,t)\}. \tag{7}$$

Eq. (7) represents the difference between a pixel's intensity at coordinates (x,y) and the mean of all pixel intensities in the window.

$$g_4(x,y) = \operatorname*{std}_{(s,t)\in S^3_{x,y}} \{I(s,t)\}. \tag{8}$$

Eq. (8) represents the standard deviation of all the pixel intensities within the window.

$$g_5(x,y) = I(x,y). \tag{9}$$

Eq. (9) is the gray intensity of the center pixels (x,y) of the window.

After computing each pixel of the ROI with coordinates (x,y) and the five gray-level features g_i, $i = 1, \ldots, 5$, we obtain their mean, defined by the following formula:

$$G_i = \operatorname*{mean}_{(x,y)} g_i(x,y) = E(g_i) = \frac{1}{N}\sum_{j=1}^{N} g_i\left(x_j, y_j\right), \tag{10}$$

for each $i = 1, \ldots, 5$, where E denotes the expected value, and N is the total number of pixels in the ROI.

Finally, we consider the demographic variables "age" and "gender" of each patient, and we the collect features previously described into a set entitled F1, which includes 14 features:

$mean_r$, $mean_g$, $mean_b$, $mean_{r-g}$, HHR, Ent, B, Age, $Gender$, G_i, $i = 1, \ldots, 5$.

All the features extracted from the segmented conjunctiva images, except those obtained from the gray-level features $g_1, \ldots, g_5$, were obtained after removing all the pixels whose components in the RGB color space were less than or equal to 20 and greater than or equal to 240. In other words, we only consider the pixels from the segmented conjunctival images whose RGB components satisfy the following relation:

$$(20,20,20)\langle(r_i,g_i,b_i)\langle(240,240,240),$$

where r_i, g_i and b_i represent the red, green, and blue components of the ith pixel of the segmented conjunctiva image, respectively.

Following [39], we apply this filter to remove pixels that are too dark or too light. In particular, we choose the minimum and maximum values of 20 and 240, respectively, which are the approximate values of those suggested by the authors in [39].

Most of the selected features are pixel statistics, which are closely related to image quality. We did not perform any denoising and instead worked with the images captured by the device. Images in the dataset were acquired under controlled conditions. As shown in Fig. 2, the acquired images were of high quality and large size.

The image acquisition prototype consisted of a smartphone, macrolens, and special spacer. The macrolens, which is enclosed in the spacer as shown in Fig. 1, makes it possible to take very close-up photos of the ROI, allowing you to see tiny details. The spacer is designed so as to easily place it around the area of the eye and, due to its suitable slant, allows the camera to take a photo that is precisely focused on the eyelid conjunctiva; Fig. 4 shows a photo of the spacer and two design drawings. This model has been registered with the Italian Patent and Trademark Office (No. 402019000001958). The macro lens was located inside the hole visible in the photo. The prototype in Fig. 4 was 3D printed in PLA material with a base width of 2.5 in. LED lights are mounted around the spacer (see Fig. 1); thus, this device is insensitive to ambient light and can capture high-resolution pictures of the conjunctiva. The design of the internal lighting of the acquisition device makes it possible to minimize reflection owing to the moistness of the eye. Under these conditions, specific denoising was not necessary, and the images were clean and homogeneous. The only filtering performed is described above, and its goal is to exclude image pixels that do not carry useful color information, for example, those that are too light (residual reflections) or too dark, such as shadows in the peripheral area of the conjunctiva, eyelashes, and even a small nevus of the conjunctiva in one case.

3.3. RUSBoost

Class imbalance, which occurs when one class is less represented than others, frequently occurs in several applications. In this study, there

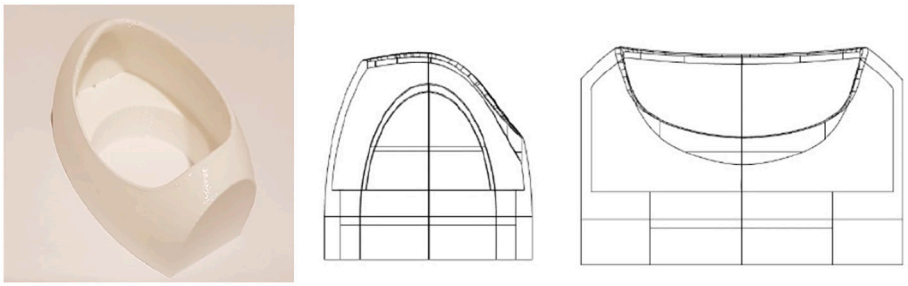

Fig. 4. Details of the spacer.

were fewer anemic than non-anemic patients in all datasets. This problem can degrade the performance of the classification algorithms. This is a very common problem in medicine, particularly in the case of rare diseases.

RUSBoost [56,71], is a hybrid sampling and boosting algorithm that combines random undersampling (RUS) and AdaBoost to address class imbalance. The data-sampling technique RUS randomly removes examples from the majority class until the cardinality of the majority and minority classes becomes the same. AdaBoost is a boosting algorithm used to improve the classification performance of weak classifiers; initially, all examples in the training set have the same weights. During each AdaBoost iteration, the weak learner formed a weak hypothesis. After calculating the error associated with this hypothesis, the weight of each data point was adjusted so that the weights of the misclassified examples increased. In contrast, the weights of the correctly classified examples decreased. Therefore, subsequent boosting iterations will generate more likely hypotheses to accurately classify previously mislabeled examples. After all iterations were completed, a weighted vote of all the hypotheses was used to assign a class to the unlabeled examples.

In RUSBoost, the RUS algorithm helps balance the class distribution, and the AdaBoost algorithm improves the performance of the base learner using balanced data. In the first step of the algorithm, the weight of each example was initialized to the reciprocal of the cardinality of the training set. Then, the weak hypothesis is trained several times, equal to the number of classifiers in the ensemble. Here, RUS is applied such that the majority and minority class examples are equal. As a result, the new temporary training set will have a new weight distribution. Then, the new training set and the distribution of the new weights are passed on to the base learner, which creates a weak hypothesis. The pseudoloss based on the original training set and original weight distribution is calculated and used to obtain the updated weight parameter. Next, the weight distribution for the following iteration was updated and normalized. When the total number of iterations was complete, the final hypothesis was given by a weighted vote of the weak hypotheses.

3.4. Evaluation metrics

To evaluate the performance of the classification algorithms, we used the evaluation metrics from the confusion matrix. The conjunctiva images that the classifier correctly identified as belonging to the anemic class represented the true positive (TP), and the images correctly identified as not anemic represented the true negative (TN). The conjunctival images of non-anemic patients incorrectly classified as belonging to the anemic class were false positives (FPs). Finally, the conjunctival images of anemic patients incorrectly identified as belonging to the nonanemic class were false negatives (FNs). Based on these notations, accuracy, sensitivity, and specificity are defined as follows:

$$Accuracy = \frac{TP + TN}{TP + FN + FP + TN}$$

$$Sensitivity = \frac{TP}{TP + FN}$$

$$Specif\ \ icity = \frac{TN}{FP + TN}$$

These metrics were computed in each run of the cross-validation process, and the performance of the classifier was assessed by the average and standard deviation of the values obtained.

The accuracy metric, although in many cases a good estimate of a system's performance, should not be considered too reliable due to the imbalance of the two classes in the dataset. Since the goal of a system such as that proposed in this study is initial screening focused on bringing a patient who was not aware of being anemic to carry out deeper investigations, it was decided to prioritize sensitivity, which expresses, as a percentage, how many of the actual anemic patients were detected by the system.

4. Experiments and results

Experiments were performed using MATLAB R2021a with the ThinkStation P620, model 30E0CTO1WW, CPU AMD Threadripper Pro 3975WX, RDIMM ECC DDR4–3.200 MHz–64 GB, and NVIDIA Quadro RTX 5000, 16 GB.

The support system for anemia detection is based on RUSBoost [56,71] and is used to establish whether each conjunctiva image belongs to an anemic patient using the set of features F1. In all experiments, we used holdout cross-validation (CV) with 200 iterations (50 in the case of MobileNet). In each run of the CV, the dataset was randomly split into exactly two subsets of specified ratios for training (70 %) and testing (30 %), while preserving the proportion of anemic and non-anemic patients in each subset (in the Deep Learning case, the ratios were 70 % for training, 15 % for validation, and 15 % for testing). For each conjunctiva's image, we assign the label “1” if the patient is anemic (i.e., if their Hb concentration is less than or equal to 10.5 g/dL) and “0” otherwise. Finally, the trained classifier was tested on the test set in each round of cross-validation, and the evaluation metrics (Section 3.4) were computed in each run of the cross-validation. Subsequently, the model's performance was assessed by utilizing the average and standard deviation of the metrics computed over CV runs.

Table 2
RUSBoost on each dataset with 200 CV and a cutoff of Hb $\leq$ 10.5 g/dL. For all the metrics, the mean $\pm$ standard deviation computed over the round of cross-validation are reported.

RUSBoost			
Dataset	Evaluation metrics	Whole conjunctiva	Palpebral conjunctiva
Italian	Accuracy	0.87 ± 0.06	0.88 ± 0.05
	Sensitivity	0.64 ± 0.32	0.66 ± 0.29
	Specificity	0.90 ± 0.07	0.91 ± 0.06
Indian	Accuracy	0.77 ± 0.07	0.75 ± 0.07
	Sensitivity	0.70 ± 0.15	0.79 ± 0.18
	Specificity	0.80 ± 0.11	0.74 ± 0.10
Joint	Accuracy	0.83 ± 0.04	0.83 ± 0.04
	Sensitivity	0.66 ± 0.16	0.69 ± 0.15
	Specificity	0.87 ± 0.06	0.87 ± 0.06

The experimental results showed that the RUSBoost algorithm achieved good performance on all datasets (see Table 2). The performances achieved by RUSBoost using palpebral conjunctiva images are almost always better than those obtained considering the pictures of the entire conjunctiva for both Italian and Indian patient eye image datasets, confirming that the palpebral conjunctiva is a suitable tissue to detect the presence of anemia. In fact, the detection accuracy of the system on the palpebral conjunctiva was 88 % for the Italian patient eye image dataset and 75 % for the Indian patient eye image dataset. The sensitivity (i.e., the proportion of patients who had an anemic condition and received a positive test result) of the RUSBoost algorithm on the palpebral conjunctiva of the Indian patient eye image dataset (79 %) was better than that of the Italian patient eye image dataset (66 %). In general, when compared with performances on the Italian patient eye image dataset, the performance of the support system on the Indian patient eye image dataset is more balanced among anemic and non-anemic patients, with a sensitivity and specificity of 79 % and 74 %, respectively. This result may have occurred because of the availability of a higher number of Indian anemic patients (31) than Italian anemic patients (11) and a more severe class imbalance in the Italian patient eye image dataset (Italian anemic patients represent 9.5 % of the entire dataset) than in the Indian patient eye image dataset (Indian anemic patients represent 32.6 % of the entire dataset).

Finally, the joint dataset obtained from the whole and palpebral conjunctiva images of Italian and Indian patients was used to train the support system with RUSBoost. This dataset had a 19.9 % class imbalance, and the system performed well on the palpebral conjunctiva, achieving an accuracy of 83 %, a sensitivity of 69 %, and a specificity of 87 %. These results suggest that the class imbalance has an impact on the automated detection of anemia.

To compare, we also developed a support system using random forest [56,92] using the same parameter settings as RUSBoost. The experimental results of the random forest for each dataset are listed in Table 3, confirming that RUSBoost is suitable for alleviating the problem of data imbalance [71] and is the optimal choice for anemia detection using the two available datasets.

The accuracy of Random Forest is better than that of RUSBoost, although RUBoost sensitivity is much higher than that of Random Forest. The reason for this phenomenon is that RUSBoost was designed to treat unbalanced datasets and has shown very high performance in these cases in the literature. This is because the algorithm implemented in RUSBoost achieves higher sensitivities than Random Forest; that is, RUSBoost performs significantly better than Random Forest in the minority class when the imbalance is high.

As mentioned above, we chose to prioritize sensitivity, which expresses the percentage of the actual anemic patients that the system was able to detect.

For further comparison, we developed a system with SVM and kNN classifiers using the same procedure. The experimental results are presented in Tables 4 and 5. The discussion above can also be considered analogous to the comparison with these two last classifiers.

Table 3
Random Forest on each dataset with 200 CV and a cutoff Hb $\leq$ 10.5 g/dL. For all the metrics, the mean $\pm$ standard deviation computed over the round of cross-validation are reported.

Random Forest			
Dataset	Evaluation metrics	Whole conjunctiva	Palpebral conjunctiva
Italian	Accuracy	0.90 $\pm$ 0.02	0.91 $\pm$ 0.02
	Sensitivity	0.14 $\pm$ 0.21	0.19 $\pm$ 0.24
	Specificity	0.97 $\pm$ 0.03	0.98 $\pm$ 0.03
Indian	Accuracy	0.80 $\pm$ 0.06	0.76 $\pm$ 0.06
	Sensitivity	0.64 $\pm$ 0.15	0.61 $\pm$ 0.20
	Specificity	0.88 $\pm$ 0.08	0.83 $\pm$ 0.11
Joint	Accuracy	0.85 $\pm$ 0.03	0.84 $\pm$ 0.03
	Sensitivity	0.51 $\pm$ 0.16	0.49 $\pm$ 0.17
	Specificity	0.93 $\pm$ 0.04	0.93 $\pm$ 0.05

Table 4
SVM classifier on each dataset with 200 CV and a cutoff Hb $\leq$ 10.5 g/dL. For all the metrics, the mean $\pm$ standard deviation computed over the round of cross-validation are reported.

SVM			
Dataset	Evaluation metrics	Whole conjunctiva	Palpebral conjunctiva
Italian	Accuracy	0.90 $\pm$ 0.04	0.92 $\pm$ 0.03
	Sensitivity	0.46 $\pm$ 0.30	0.46 $\pm$ 0.29
	Specificity	0.94 $\pm$ 0.04	0.96 $\pm$ 0.03
Indian	Accuracy	0.80 $\pm$ 0.06	0.79 $\pm$ 0.06
	Sensitivity	0.75 $\pm$ 0.14	0.71 $\pm$ 0.15
	Specificity	0.82 $\pm$ 0.08	0.83 $\pm$ 0.08
Joint	Accuracy	0.86 $\pm$ 0.03	0.87 $\pm$ 0.03
	Sensitivity	0.64 $\pm$ 0.12	0.62 $\pm$ 0.13
	Specificity	0.91 $\pm$ 0.04	0.93 $\pm$ 0.03

Table 5
kNN classifier on each dataset with 200 CV and a cutoff Hb $\leq$ 10.5 g/dL. For all the metrics, the mean $\pm$ standard deviation computed over the round of cross-validation are reported.

kNN			
Dataset	Evaluation metrics	Whole conjunctiva	Palpebral conjunctiva
Italian	Accuracy	0.90 $\pm$ 0.04	0.90 $\pm$ 0.03
	Sensitivity	0.42 $\pm$ 0.28	0.38 $\pm$ 0.25
	Specificity	0.95 $\pm$ 0.06	0.95 $\pm$ 0.03
Indian	Accuracy	0.72 $\pm$ 0.06	0.63 $\pm$ 0.07
	Sensitivity	0.58 $\pm$ 0.15	0.45 $\pm$ 0.15
	Specificity	0.80 $\pm$ 0.08	0.71 $\pm$ 0.09
Joint	Accuracy	0.83 $\pm$ 0.04	0.78 $\pm$ 0.04
	Sensitivity	0.53 $\pm$ 0.13	0.46 $\pm$ 0.13
	Specificity	0.90 $\pm$ 0.04	0.86 $\pm$ 0.05

In the preliminary stage, we also experimented with a deep learning technique, but it did not provide convincing results. CNN and deep learning techniques require many images, which are not available, and we have also resorted to data augmentation techniques. The results obtained using MobileNet-V2 are listed in Table 6.

There could also be an explanation for this specific case: deep learning can turn out to be less efficient when the information is sufficiently hidden, as in the situation at hand, where even for humans it is difficult to diagnose anemia from an image of the conjunctiva due to the subtle differences in pallor between the two states.

5. Conclusions and open questions

Screening for anemia using noninvasive and cost-effective devices is currently a significant research challenge because it spares patients the discomfort of physical examinations and ensures savings for the national

Table 6
MobileNet-V2 on each dataset with 50 CV and cutoff of Hb $\leq$ 10.5 g/dL. For all the metrics, the mean $\pm$ standard deviation computed over the round of cross-validation are reported. (Max epochs: 30, learning rate: (3 $\times$ 10)^(−4), optimizer: SGD.)

MobileNet-V2			
Dataset	Evaluation metrics	Whole conjunctiva	Palpebral conjunctiva
Italian	Accuracy	0.91 $\pm$ 0.05	0.91 $\pm$ 0.06
	Sensitivity	0.24 $\pm$ 0.35	0.44 $\pm$ 0.45
	Specificity	0.97 $\pm$ 0.04	0.97 $\pm$ 0.06
Indian	Accuracy	0.68 $\pm$ 0.12	0.64 $\pm$ 0.09
	Sensitivity	0.46 $\pm$ 0.26	0.41 $\pm$ 0.24
	Specificity	0.78 $\pm$ 0.14	0.76 $\pm$ 0.13
Joint	Accuracy	0.82 $\pm$ 0.06	0.83 $\pm$ 0.06
	Sensitivity	0.49 $\pm$ 0.21	0.52 $\pm$ 0.21
	Specificity	0.90 $\pm$ 0.06	0.90 $\pm$ 0.06

health program. A considerable number of recent studies have demonstrated the relevance of excitement in this sector; however, many problems remain unsolved. One of these is the lack of a widely used and approved automatic system for the diagnosis of anemia among doctors. Moreover, the most suitable data (i.e., pallor of the palms of the hands, fingertips, nail beds, or eye conjunctiva) for use in these automated systems have not been officially recognized in the literature, and open questions also consider the features to be extracted from those data to optimize the performance of the automated diagnosis.

With reference to data sharing, many publishers provide a data platform that supports open data initiatives and gives everyone the opportunity to manage, share, access, and store research data, particularly in medicine. Data sharing would provide all researchers with the opportunity to freely access all shared datasets and be able to analyze and use them, or even increase and improve them. In this regard, the publication of the dataset containing the eye images of Italian and Indian patients used in the experiments is a significant contribution of this study.

Another main contribution of this work is the development of a novel decision support system with the RUSBoost classifier devoted to anemia detection and trained on Italian and Indian datasets. The system was trained using conjunctiva selected from the eye images collected from these datasets. In fact, the high number of microvessels makes the conjunctiva a perfect candidate for estimating pallor. In particular, the palpebral conjunctiva highlights the vascularization of the underlying area compared to the forniceal conjunctiva, allowing us to better appreciate even the slightest shades of blood color. In particular, the palpebral and whole conjunctiva were used to train the proposed decision support system, and the results highlighted that the palpebral conjunctiva had the best performance on the two datasets. The proposed system is also successfully able to treat an imbalance in the available number of examples from anemic patients compared to controls. In fact, the system, trained using palpebral conjunctiva, showed an accuracy of 88 % (sensitivity = 0.66, specificity = 0.91) on the Italian dataset and 75 % (sensitivity = 0.79, specificity = 0.74) on the Indian dataset. Finally, we tested the system on the joint dataset and obtained good performance, comparable to the previous, demonstrating that the system is also robust to the variability introduced by the different ethnicities considered.

In general, the system performance was good. It is of little significance to compare the results obtained with different datasets and experimental sets that are not homogeneous. Instead of offering comparisons with other studies, it is useful to define and propose a common experimental basis. We think that this study is not 'just another one'; rather, it could be considered as a new starting point for the community working on this topic, and other researchers could contest our research with the aim of obtaining better results.

Some of the factors worth examining in future studies to improve performance in classifying anemic and non-anemic patients are the intrinsic characteristics of the patients, such as other symptoms and pathologies reported in anamnesis, which would allow the system to be calibrated to the individual patient, enabling a more accurate classification and thus estimation of the presence of the pathology. We are currently studying the changes in pallor that the conjunctiva undergoes when the Hb concentration in the blood varies in cancer patients using the temporal series of data from the same individuals.

We believe that the results of this study will allow us to identify the factors needed to better calibrate the method and/or device on an individual patient, enabling the system to better recognize the characteristic traits of an anemic patient.

Moreover, further studies should focus on the opportunity to use different types of data (i.e., pallor of the palms of the hands and eye conjunctiva) to build classifiers while simultaneously solving multiple learning tasks at the same time.

Conflict of interest

The authors declare the absence of any potential competing interests in a person or entity of a financial, non-financial, professional or personal nature, or interests that may be perceived as such, in connection with the research.

We declare the absence of competing potential to the best of our knowledge and belief.

Appendix 1

Eyes-defy-anemia dataset short description

The Eyes-defy-anemia dataset contains 218 images of eyes, particularly conjunctivas, which can be used for research on the diagnosis/estimation of anemia based on the pallor of the conjunctiva.

The same images can be effectively used to study segmentation algorithms of the conjunctiva or the exposed parts of the sclera and iris. All images of the dataset were accompanied by segmented elements (palpebral, forniceal, and palpebral + forniceal conjunctivas), useful both to directly correlate the pallor with the value of Hb and to assess the performance of segmentation algorithms. Each image is accompanied by essential information, such as the value of Hb measured in the laboratory and the age and sex of the patient, as listed in thexlsx files.

The images were captured using a Samsung smartphone equipped with a device that magnifies images, standardizes lighting, and eliminates the influence of ambient light. Therefore, all images were captured at the same distance with the same white LED light. A description of the acquisition set is included in our papers linked to the dataset.

IMPORTANT NOTE: Segmentation of the parts of the eye was carried out by experienced personnel according to their own interpretation. Every user of the images of the dataset can use our segmentations or use the whole images of the eye and segment them as they see fit.

The dataset Eyes-defy-anemia was divided into two folders, one for Italian patients and one for Indian patients.

Folder Italy contains 123 folders and an Italy. xlsx file. The name of the folder, from 1 to 123, refers to the number contained in the "Number" field of the Italy. xlsx file. Within each numbered folder, there are four files.

file name.jpg, representing the original eye
- forniceal_palpebral.png: image depicting two conjunctives segmented by hand.
- forniceal.png: image depicting the forniceal conjunctiva segmented by hand
- palpebral.png: image depicting the palpebral conjunctiva segmented by hand.

The exception are folders labeled as 1, 35, 54, 58, 75, and 109; in fact, in these images of the eye, the forniceal conjunctiva is not exposed, so in these folders only 2 files are available:

file name.jpg, representing the original eye
- palpebral.png: image depicting the palpebral conjunctiva segmented by hand.

The Hgb level for patient 93 was not recorded; however, we consider it useful to make the four images listed above available to the scientific community.

All the images of the eye were acquired in Bari (Italy).

The India folder contains 95 folders and the India.xls file.

The folder name, from 1 to 95, includes a number that corresponds to the "Number" field of the file India.xlsx.

Within each numbered folder there are 4 files:

file name.jpg, representing the original eye

- forniceal_palpebral.png: image depicting the two conjunctivas segmented by hand
- forniceal.png: image depicting the forniceal conjunctiva segmented by hand
- palpebral.png: image depicting the palpebral conjunctiva segmented by hand.

All images of the eye were acquired in Karapakkam, Chennai (India).

All images obtained after segmentation were RGB images of equal size (1067 × 800 pixels).

References

[1] De Benoist B., Cogswell M., Egli I., McLean E. Worldwide prevalence of anaemia 1993–2005: WHO global database on anaemia. WHO Glob. Database Anaemia 2008. ISBN 9789241596657. [Online]. Available: https://apps.who.int/iris/handle/10665/43894.

[2] WHO. Assessing the iron status of populations: including literature reviews: report of a Joint World Health Organization/Centers for Disease Control and Prevention [Online]. Available. Geneva, Switzerland: World Health Organization; 2004. https://apps.who.int/iris/handle/10665/75368.

[3] McLean E, Cogswell M, Egli I, Wojdyla D, De Benoist B. Worldwide prevalence of anaemia, WHO vitamin and mineral nutrition information system, 1993–2005. Public Health Nutr Apr. 2009;12(4):444–54. https://doi.org/10.1017/S1368980008002401.

[4] "World health organization micronutrient deficiencies,"n.d.. Available online: http://www.who.int/nutrition/topics/ida/en/.

[5] Who. The world health report 2002 - reducing risks, promoting healthy life. Educ. Health Change Learn. Pract. Jan. 2003;16(2). https://doi.org/10.1080/1357628031000116808. 230 230.

[6] Patel KV. Epidemiology of anemia in older adults. Semin Hematol Oct. 2008;45(4):210–7. https://doi.org/10.1053/j.seminhematol.2008.06.006.

[7] Porwit A, McCullough J, Erber WN. Blood and bone marrow pathology. Elsevier Ltd; 2011 [Online]. Available:.

[8] Benseñor IM, Calich ALGarcia, Brunoni ARussowsky, do Espírito-Santo FFerreira, Mancini RLendimuth, Drager LFerreira, Lotufo PAndrade. Accuracy of anemia diagnosis by physical examination. Sao Paulo Med. J. Rev. Paul. Med. May 2007;125(3):170–3. https://doi.org/10.1590/s1516-31802007000300008.

[9] Tsumura N, Ojima N, Sato K, Shiraishi M, Shimizu H, Nabeshima H, Akazaki S, Hori K, Miyake Y. Image-based skin color and texture analysis/synthesis by extracting hemoglobin and melanin information in the skin. ACM Trans Graph 2003. https://doi.org/10.1145/1201775.882344.

[10] Angelopoulou E. Understanding the color of human skin. Human Vision and Electronic Imaging VI Jun. 2001;4299:243–51. https://doi.org/10.1117/12.429495.

[11] Spinelli MGN, Souza JMP, de Souza SB, Sesoko EH. Reliability and validity of palmar and conjunctival pallor for anemia detection purposes. Rev. Saúde Pública Aug. 2003;vol. 37, no. 4, Art. no. 4. https://doi.org/10.1590/S0034-89102003000400003.

[12] Kalter HD, Burnham G, Kolstad PR, Hossain M, Schillinger JA, Khan NZ, Saha S, de Wit V, Kenya-Mugisha N, Schwartz B, Black RE. Evaluation of clinical signs to diagnose anaemia in Uganda and Bangladesh, in areas with and without malaria. Bull World Health Organ 1997;75(Suppl 1):103–11.

[13] Sheth TN, Choudhry NK, Bowes M, Detsky AS. The relation of conjunctival pallor to the presence of anemia. J Gen Intern Med 1997;2(12):102–6. https://doi.org/10.1007/s11606-006-5004-x.

[14] da Silva RM, Machado CA. Clinical evaluation of the paleness: agreement between observers and comparison with hemoglobin levels. Rev. Bras. Hematol. E Hemoter. 2010;32:444–8. https://doi.org/10.1590/S1516-84842010000600007.

[15] Dusch E, Galloway R, Achadi E, et al. Clinical screening may be a cost-effective way to screen for severe anaemia. Food Nutr Bull 1999;20(4):409–16. https://doi.org/10.1177/156482659902000404.

[16] Dimauro G, Caivano D, Di Pilato P, Dipalma A, Camporeale MG. A systematic mapping study on research in anemia assessment with non-invasive devices. Appl. Sci. Jan. 2020;10(14):14. https://doi.org/10.3390/app10144804.

[17] Ughasoro MD, Madu AJ, I. C. Kela -Eke. Clinical anaemia detection in children of varied skin complexion: a community-based study in southeast, Nigeria. J. Trop. Pediatr. Feb. 2017;63(1):23–9. https://doi.org/10.1093/tropej/fmw044.

[18] Butt Z, Ashfaq U, Sherazi SFH, Jan NU, Shahbaz U. Diagnostic accuracy of "pallor" for detecting mild and severe anaemia in hospitalized patients. JPMA J. Pak. Med. Assoc. Sep. 2010;60(9):762–5.

[19] Kalantri A, Karambelkar M, Joshi R, Kalantri S, Jajoo U. Accuracy and reliability of pallor for detecting anaemia: a hospital-based diagnostic accuracy study. PLOS ONE Jan. 2010;5(1):e8545. https://doi.org/10.1371/journal.pone.0008545.

[20] Yurdakök K, Güner SN, Yalçin SS. Validity of using pallor to detect children with mild anemia. Pediatr. Int. Off. J. Jpn. Pediatr. Soc. Apr. 2008;50(2):232–4. https://doi.org/10.1111/j.1442-200X.2008.02565.x.

[21] Bergsjø P, Evjen-Olsen B, Hinderaker SG, Oleking'ori N, Klepp K-I. Validity of non-invasive assessment of anaemia in pregnancy. Feb Trop. Med. Int. Health TM IH 2008;13(2):272–7. 10.1111/j.1365-3156.2007.02000.x.

[22] Suner S, Rayner J, Ozturan IU, Hogan G, Meehan CP, Chambers AB, Baird J, Jay GD. Prediction of anemia and estimation of hemoglobin concentration using a smartphone camera. PLOS ONE Jul. 2021;16(7):e0253495. https://doi.org/10.1371/journal.pone.0253495.

[23] Rivero-Palacio M, Alfonso-Morales W, Caicedo-Bravo E. Mobile application for anemia detection through ocular conjunctiva images. In: 2021 IEEE Colombian conference on applications of computational intelligence (ColCACI); May 2021. p. 1–6. https://doi.org/10.1109/ColCACI52978.2021.9469593.

[24] Kobayashi N, Yoshino A, Ishikawa M, Homma S. Anemia examination using a hyperspectral camera in telecare system. In: Presented at 2021 IEEE 3rd Global Conference on Life Sciences and Technologies (LifeTech); 2021. p. 475–6. https://doi.org/10.1109/LifeTech52111.2021.9391912. Mar.

[25] Fuadah YN, Sa'idah S, Wijayanto I, Patmasari R, Magdalena R. Non invasive anemia detection in pregnant women based on digital image processing and K-nearest neighbor. In: Presented at 2020 3rd international conference on biomedical engineering (IBIOMED); Oct. 2020. p. 60–4. https://doi.org/10.1109/IBIOMED50285.2020.9487605.

[26] Jain P, Bauskar S, Gyanchandani M. Neural network based non-invasive method to detect anemia from images of eye conjunctiva. Int. J. Imaging Syst. Technol. 2020;30(1):112–25. https://doi.org/10.1002/ima.22359.

[27] Kasiviswanathan S, Vijayan TB, John S. Ridge regression algorithm based non-invasive anaemia screening using conjunctiva images. J. Ambient Intell. Humaniz. Comput. Oct. 2020. https://doi.org/10.1007/s12652-020-02618-3.

[28] Bauskar S, Jain P, Gyanchandani M. A noninvasive computerized technique to detect anemia using images of eye conjunctiva. Pattern Recognit Image Anal Jul. 2019;29(3):438–46. https://doi.org/10.1134/S1054661819030027.

[29] Sharma M, Garg B. Non-invasive anaemia detection by analysis of conjunctival pallor. In: Advanced Computational and Communication Paradigms, Lecture Notes in Electrical Engineering. 475. Singapore: Springer; 2018. p. 224–31.

[30] Roychowdhury S, Sun D, Bihis M, Ren J, Hage P, Rahman HH. Computer aided detection of anemia-like pallor. In: Presented at 2017 IEEE EMBS international conference on biomedical health informatics (BHI); Feb. 2017. p. 461–4. https://doi.org/10.1109/BHI.2017.7897305.

[31] Sarkar PK, et al. Development and validation of a noncontact spectroscopic device for hemoglobin estimation at point-of-care. J Biomed Opt May 2017;22(5):055006. https://doi.org/10.1117/1.JBO.22.5.055006.

[32] Kim O, McMurdy J, Jay G, Lines C, Crawford G, Alber M. Combined reflectance spectroscopy and stochastic modeling approach for noninvasive hemoglobin determination via palpebral conjunctiva. Physiol Rep 2014;2(1):e00192. https://doi.org/10.1002/phy2.192.

[33] McMurdy JW, Jay GD, Suner S, Crawford GP, Crawford GP, Trespalacios. Anemia detection utilizing diffuse reflectance spectra from the palpebral conjunctiva and tunable liquid crystal filter technology. In: Health monitoring and smart nondestructive evaluation of structural and biological systems V. 6177; Mar. 2006. p. 403–12. https://doi.org/10.1117/12.657883.

[34] McMurdy JW, Jay GD, Suner S, Trespalacios FM, Crawford GP. Diffuse reflectance spectra of the palpebral conjunctiva and its utility as a noninvasive indicator of total hemoglobin. J Biomed Opt Jan. 2006;11(1):014019. https://doi.org/10.1117/1.2167967.

[35] Meda N, Dao Y, Touré B, Yameogo B, Cousens S, Graham W. Evaluer l'anémie maternelle sévère et ses conséquences: la valeur d'un simple examen de la coloration des conjonctives palpébrales [Assessing severe maternal anemia and its consequences: the value of a simple examination of the coloration of palpebral conjunctiva]. Sante. Montrouge Fr. 1999;9(1):12–7. Feb.

[36] Dimauro G, Guarini A, Caivano D, Girardi F, Pasciolla C, Iacobazzi A. Detecting clinical signs of anaemia from digital images of the palpebral conjunctiva. IEEE Access 2019;7:113488–98. https://doi.org/10.1109/ACCESS.2019.2932274.

[37] Sevani N, Persulessy GBV, Fredicia. Detection anemia based on conjunctiva pallor level using k-means algorithm. IOP Conf. Ser. Mater. Sci. Eng. Oct. 2018;420:012101. https://doi.org/10.1088/1757-899X/420/1/012101.

[38] Tamir A, Jahan CS, Saif MS, Sums SU, Islam MdM, Khan AI, Fattah SA, Anowarul Shaikh, Shahnaz C. Detection of anemia from image of the anterior conjunctiva of the eye by image processing and thresholding. In: 2017 IEEE Reg. 10 Humanit. Technol. Conf. R10-HTC; 2017. https://doi.org/10.1109/R10-HTC.2017.8289053.

[39] Dimauro G, Caivano D, Girardi F. A new method and a non-invasive device to estimate anemia based on digital images of the conjunctiva. IEEE Access 2018;6:46968–75. https://doi.org/10.1109/ACCESS.2018.2867110.

[40] Collings S, Thompson O, Hirst E, Goossens L, George A, Weinkove R. Non-invasive detection of anaemia using digital photographs of the conjunctiva. PLOS ONE Apr. 2016;11(4):e0153286. https://doi.org/10.1371/journal.pone.0153286.

[41] Chen YM, Miaou SG, Bian H. Examining palpebral conjunctiva for anemia assessment with image processing methods. Comput Methods Programs Biomed Dec. 2016;137:125–35. https://doi.org/10.1016/j.cmpb.2016.08.025.

[42] Chen YM, Miaou SG. A Kalman filtering and nonlinear penalty regression approach for noninvasive anemia detection with palpebral conjunctiva images. J. Healthc. Eng. Jul. 2017;2017:e9580385. https://doi.org/10.1155/2017/9580385.

[43] Bevilacqua V, Dimauro G, Marino F, Brunetti A, Cassano F, Maio ADi, Nasca E, Trotta GF, Girardi F, Ostuni A, Guarini A, Guarini A. A novel approach to evaluate blood parameters using computer vision techniques. In: 2016 IEEE international symposium on medical measurements and applications (MeMeA); May 2016. p. 1–6. https://doi.org/10.1109/MeMeA.2016.7533760.

[44] Hasan MK, Haque M, Sakib N, Love R, Ahamed SI. Smartphone-based human hemoglobin level measurement analyzing pixel intensity of a fingertip video on different color spaces. Smart Health Jan. 2018;5–6:26–39. https://doi.org/10.1016/j.smhl.2017.11.003.

[45] Hasan MK, Haque MM, Adib R, Tumpa JF, Begum A, Love RR, Kim YL, Sheikh IA. SmartHeLP: smartphone-based hemoglobin level prediction using an artificial neural network. AMIA Annu Symp Proc AMIA Symp 2018;2018:535–44.
[46] Mannino RG, Myers DR, Tyburski EA, Caruso C, Boudreaux J, Leong T, Clifford GD, Lam Wilbur A. Smartphone app for non-invasive detection of anemia using only patient-sourced photos. Nat Commun Dec. 2018;9(1):4924. https://doi.org/10.1038/s41467-018-07262-2.
[47] Hasan MK, Sakib N, Love RR, Ahamed SI. Analyzing the existing noninvasive hemoglobin measurement techniques. In: 2017 IEEE 8th annual ubiquitous computing, electronics and mobile communication conference (UEMCON); Oct. 2017. p. 442–8. https://doi.org/10.1109/UEMCON.2017.8249080.
[48] Ahsan GMT, Gani MO, Hasan MK, Ahamed SI, Chu W, Adibuzzaman M, Joshua F. A novel real-time non-invasive hemoglobin level detection using video images from smartphone camera. In: 2017 IEEE 41st annual computer software and applications conference (COMPSAC). 1; Jul. 2017. p. 967–72. https://doi.org/10.1109/COMPSAC.2017.29.
[49] Hasan MK, Sakib N, Field J, Love RR, Ahamed SI. A novel process to extract important information from invisible video captured by smartphone. In: 2017 IEEE great lakes biomedical conference (GLBC); Apr. 2017. https://doi.org/10.1109/GLBC.2017.7928878. pp. 1–1.
[50] Ancona N, Maglietta R, Stella E. Data representations and generalization error in kernel based learning machines. Pattern Recognit Sep. 2006;39(9):1588–603. https://doi.org/10.1016/j.patcog.2005.11.025.
[51] Maglietta R, Milella A, Caccia M, Bruzzone G. A vision-based system for robotic inspection of marine vessels. Signal Image Video Process. Mar. 2018;12(3):471–8. https://doi.org/10.1007/s11760-017-1181-9.
[52] Yin J, Zhao W. Fault diagnosis network design for vehicle on-board equipments of high-speed railway. Eng Appl Artif Intel Nov. 2016;56(C):250–9. https://doi.org/10.1016/j.engappai.2016.10.002.
[53] Balakrishnan N, Devasigamani AI, Anupama KR, Sharma N. Aero-engine health monitoring with real flight data using whale optimization algorithm based artificial neural network technique. Opt Mem Neural Netw Jan. 2021;30(1):80–96. https://doi.org/10.3103/S1060992X21010094.
[54] Gulzar Y, Hamid Y, Soomro AB, Alwan AA, Journaux L. A convolution neural network-based seed classification system. Symmetry 2020;12(12):12. https://doi.org/10.3390/sym12122018. Dec.
[55] Inglese P, Amoroso N, Boccardi M, Bocchetta M, Bruno S, Chincarini A, Errico R, Frisonichi GB, Maglietta R, Redolfi A, Sensi F, Tangaro S, Tateo A, Bellotti R. Multiple RF classifier for the hippocampus segmentation: method and validation on EADC-ADNI harmonized hippocampal protocol. Phys Medica PM Int J Devoted Appl Phys Med Biol Off J Ital Assoc Biomed Phys AIFB Dec. 2015;31(8):1085–91. https://doi.org/10.1016/j.ejmp.2015.08.003.
[56] Maglietta R, Amoroso N, Boccardi M, Bruno S, Chincarini A, Frisoni GB, Inglese P, Redolfi A, Tangaro S, Tateo A, Bellotti R. Automated hippocampal segmentation in 3D MRI using random undersampling with boosting algorithm. Pattern Anal Appl May 2016;19(2):579–91. https://doi.org/10.1007/s10044-015-0492-0.
[57] Zhang Y, Chen J, Tan JH, Chen Y, Chen Y, Li D, Yang L, Su J, Huan X, Che W. An investigation of deep learning models for EEG-based emotion recognition. Front Neurosci 2020;14:1344. https://doi.org/10.3389/fnins.2020.622759.
[58] Jiang L, Sun X, Mercaldo F, Santone A. DECAB-LSTM: deep contextualized attentional bidirectional LSTM for cancer hallmark classification. Knowl.-Based Syst. Dec. 2020;210:106486. https://doi.org/10.1016/j.knosys.2020.106486.
[59] Basodi S, Baykal PI, Zelikovsky A, Skums P, Pan Y. Analysis of heterogeneous genomic samples using image normalization and machine learning. BMC Genomics Dec. 2020;21(6):405. https://doi.org/10.1186/s12864-020-6661-6.
[60] Buongiorno D, Cascarano GD, De Feudis I, Brunetti A, Carnimeo L, Dimauro G, Bevilacqua V. Deep learning for processing electromyographic signals: a taxonomy-based survey. Neurocomputing Sep. 2021;452:549–65. https://doi.org/10.1016/j.neucom.2020.06.139.
[61] Nannavecchia A, Girardi F, Fina PR, Scalera M, Dimauro G. Personal heart health monitoring based on 1D convolutional neural network. J Imaging Feb. 2021;7(2):2. https://doi.org/10.3390/jimaging7020026.
[62] Mesin L, Monaco A, Cattaneo R. Investigation of nonlinear pupil dynamics by recurrence quantification analysis. Biomed Res Int 2013;2013:420509. https://doi.org/10.1155/2013/420509.
[63] Mesin L, Mokabberi F, Carlino CF. Automated morphological measurements of brain structures and identification of optimal surgical intervention for chiari I malformation. IEEE J Biomed Health Inform Nov. 2020;24(11):3144–53. https://doi.org/10.1109/JBHI.2020.3016886.
[64] Altini N, Cascarano GD, Brunetti A, De Feudis I, Buongiorno D, Rossini M, Pesce F, Gesualdo L, Bevilacqua V. A deep learning instance segmentation approach for global glomerulosclerosis assessment in donor kidney biopsies. Electronics Nov. 2020;9(11):11. https://doi.org/10.3390/electronics9111768.
[65] Cascarano GD, Loconsole C, Brunetti A, Lattarulo A, Buongiorno D, Losavio G, Di Sciascio E, Bevilacqua V. Biometric handwriting analysis to support Parkinson's disease assessment and grading. BMC Med Inform Decis Mak Dec. 2019;19(9):252. https://doi.org/10.1186/s12911-019-0989-3.
[66] Altini N, De Giosa G, Fragasso N, Coscia C, Sibilano E, Prencipe B, Hussain SM, Brunetti A, Buongiorno D, Guerriero A, Tatò IS, Brunetti G, Triggiani V, Bevilacqua V. Segmentation and identification of vertebrae in CT scans using CNN, k-means clustering and k-NN. Informatics Jun. 2021;8(2):2. https://doi.org/10.3390/informatics8020040.
[67] Noor NB, Dey M, Anwar MdS. An efficient technique of hemoglobin level screening using machine learning algorithms. In: 2019 4th International Conference on Electrical Information and Communication Technology (EICT); 2019. p. 1–6. https://doi.org/10.1109/EICT48899.2019.9068812. Dec.
[68] Noor NB, Dey M, Anwar MdS. Comparative Study Between Decision Tree, SVM and KNN to predict anaemic condition. In: 2019 IEEE International Conference on Biomedical Engineering, Computer and Information Technology for Health (BECITHCON); 2019. p. 24–8. https://doi.org/10.1109/BECITHCON48839.2019.9063188. Nov.
[69] Yadav S, Ganesh S, Das D, Venkanna U, Mahapatra R, Shrivastava AK, Chakrabarti P, Talukder AK. Suśruta: artificial intelligence and bayesian knowledge network in health care – smartphone apps for diagnosis and differentiation of anemias with higher accuracy at resource constrained point-of-care settings. In: Big Data Analytics, Cham; 2019. p. 159–75. https://doi.org/10.1007/978-3-030-37188-3_10.
[70] Dimauro G, De Ruvo S, Di Terlizzi F, Ruggieri A, Volpe V, Colizzi L, Girardi F. Estimate of anemia with new non-invasive systems- a moment of reflection. Electronics May 2020;9(5). https://doi.org/10.3390/electronics9050780.
[71] Seiffert C, Khoshgoftaar TM, Van Hulse J, Napolitano A. RUSBoost: a hybrid approach to alleviating class imbalance. IEEE Trans Syst Man Cybern - Part Syst Hum Jan. 2010;40(1):185–97.
[72] Maglietta R, et al. Convolutional neural networks for Risso's dolphins identification. IEEE Access 2020;8:80195–206.
[73] Yalçin SS, Unal S, Gümrük F, Yurdakök K. The validity of pallor as a clinical sign of anemia in cases with beta-thalassemia. Turk J Pediatr Dec. 2007;49(4):408–12.
[74] Stoltzfus RJ, Edward-Raj A, Dreyfuss ML, Albonico M, Montresor A, Dhoj Thapa M, West KP, Chwaya HM, Savioli L, Tielsch J. Clinical pallor is useful to detect severe anemia in populations where anemia is prevalent and severe. J Nutr Sept. 1999;129(9):1675–81. https://doi.org/10.1093/jn/129.9.1675. Available:.
[75] Aggarwal AK, Tripathy JP, Sharma D, Prabhu A. Validity of palmar pallor for diagnosis of anemia among children aged 6–59 months in North India. Anemia Nov. 2014;2014:e543860. https://doi.org/10.1155/2014/543860.
[76] Nicholas C, George R, Sardesai S, Durand M, Ramanathan R, Cayabyab R. Validation of noninvasive hemoglobin measurement by pulse co-oximeter in newborn infants. J Perinatol 2015 Aug;35(8):617–20. https://doi.org/10.1038/jp.2015.12. Epub 2015 Mar 5 PMID: 25742288.
[77] Murphy SM, Omar S. The clinical utility of noninvasive pulse co-oximetry hemoglobin measurements in dark-skinned critically ill patients. Anesth Analg 2018 May;126(5):1519–26. https://doi.org/10.1213/ANE.0000000000002721. PMID: 29239951.
[78] Hennig G, Homann C, Teksan I, et al. Non-invasive detection of iron deficiency by fluorescence measurement of erythrocyte zinc protoporphyrin in the lip. Nat Commun 2016;7:10776. https://doi.org/10.1038/ncomms10776.
[79] Al-Khabori M, Al-Riyami AZ, Al-Farsi K, Al-Huneini M, Al-Hashim A, Al-Kemyani N, Daar S. Validation of a non-invasive pulse CO-oximetry based hemoglobin estimation in normal blood donors. Transfus Apher Sci 2014 Feb;50(1):95–8. https://doi.org/10.1016/j.transci.2013.10.007. Epub 2013 Nov 4 PMID: 24268769.
[80] Erdogan Kayhan G, Colak YZ, Sanli M, Ucar M, Toprak HI. Accuracy of non-invasive hemoglobin monitoring by pulse CO-oximeter during liver transplantation. Minerva Anestesiol 2017 May;83(5):485–92. https://doi.org/10.23736/S0375-9393.17.11652-4. Epub 2017 Jan 20 PMID: 28106356.
[81] Suner S, Crawford G, McMurdy J, Jay G. Non-invasive determination of hemoglobin by digital photography of palpebral conjunctiva. J Emerg Med Aug. 2007;33(2):105–11. https://doi.org/10.1016/j.jemermed.2007.02.011.
[82] Visbal-Onufrak MA, Haque MM, Were MC, Visbal-Onufrak MA, Naanyu V, Park SMok, Hasan MK, Mhawila MA, Yeung KYee, Kim YL. Virtual hyperspectral imaging of eyelids - mHematology for blood hemoglobin analysis. Available at SSRN. 2019. https://papers.ssrn.com/sol3/papers.cfm?abstract_id=3369797.
[83] Anggraeni MD, Fatoni A. Non-invasive self-care anemia detection during pregnancy using a smartphone camera. IOP Conf Ser Mater Sci Eng Feb. 2017;172:012030. https://doi.org/10.1088/1757-899X/172/1/012030.
[84] Muthalagu R, Thulasi BV, John ES. A smart (phone) solution: an effective tool for screening anemia-correlation with conjunctiva pallor and haemoglobin levels. TAGA J. Graph. Technol. 2018;14:2611–21.
[85] Irum A, Akram SAMUsman [Online]. Available. In: Anemia Detection using Image Processing; 2016. p. 31–6. http://sdiwc.net/digital-library/anemia-detection-using-image-processing.
[86] Kasiviswanathan S, Bai Vijayan T, Simone L, Dimauro G. Semantic segmentation of conjunctiva region for non-invasive anemia detection applications. Electronics Aug. 2020;9(8):8. https://doi.org/10.3390/electronics9081309.
[87] Dimauro G, Simone L. Novel biased normalized cuts approach for the automatic segmentation of the conjunctiva. Electronics Jun. 2020;9(6):6. https://doi.org/10.3390/electronics9060997.
[88] Delgado-Rivera G, Roman-Gonzalez A, Alva-Mantari A, Saldivar-Espinoza B, Zimic M, Barrientos-Porras F, Salguedo-Bohorquez M. Method for the automatic segmentation of the palpebral conjunctiva using image processing. In: 2018 IEEE international conference on automation/XXIII congress of the Chilean Association of automatic control (ICA-ACCA); Oct. 2018. p. 1–4. https://doi.org/10.1109/ICA-ACCA.2018.8609744.
[89] Setaro M, Sparavigna A. Quantification of erythema using digital camera and computer-based colour image analysis: a multicentre study. Skin Res Technol 2002;8(2):84–8. https://doi.org/10.1034/j.1600-0846.2002.00328.x.
[90] Adapa D, Raj ANJ, Alisetti SN, Zhuang Z, K. G, Naik G. A supervised blood vessel segmentation technique for digital Fundus images using Zernike Moment based

features. PLoS ONE Mar. 2020;15(3):e0229831. https://doi.org/10.1371/journal.pone.0229831.
[91] Marín D, Aquino A, Gegundez-Arias ME, Bravo JM. A new supervised method for blood vessel segmentation in retinal images by using gray-level and moment invariants-based features. IEEE Trans Med Imaging Jan. 2011;30(1):146–58. https://doi.org/10.1109/TMI.2010.2064333.
[92] Breiman L. Random forests. Mach Learn Oct. 2001;45(1):5–32. https://doi.org/10.1023/A:1010933404324.